JACS Au
AN OPEN ACCESS JOURNAL OF THE AMERICAN CHEMICAL SOCIETY

pubs.acs.org/jacsau
Article

Cell-Permeable Stimuli-Responsive Ubiquitin Probe for Time-Resolved Monitoring of Substrate Ubiquitination in Live Cells

Lu-Jun Liang,[⊥] Yu Wang,[⊥] Xiao Hua,[⊥] Rujing Yuan, Qiong Xia, Rongtian Wang, Chuntong Li, Guo-Chao Chu, Lei Liu,* and Yi-Ming Li*

Cite This: JACS Au 2023, 3, 2873−2882
Read Online
ACCESS | Metrics & More | Article Recommendations | Supporting Information

ABSTRACT: Dynamic monitoring of intracellular ubiquitin (Ub) conjugates is instrumental to understanding the Ub regulatory machinery. Although many biochemical approaches have been developed to characterize protein ubiquitination, chemical tools capable of temporal resolution probing of ubiquitination events remain to be developed. Here, we report the development of the first cell-permeable and stimuli-responsive Ub probe and its application for the temporal resolution profiling of ubiquitinated substrates in live cells. The probe carrying the photolabile group N-(2-nitrobenzyl)-Gly (Nbg) on the amide bond between Ub Gly75 and Gly76 is readily prepared through chemical synthesis and can be delivered to live cells by conjugation via a disulfide bond with the cyclic cell-penetrating peptide cR10D (i.e., 4-((4-(dimethylamino)phenyl)-azo)-benzoic acid-modified cyclic deca-arginine). Both in vitro and in vivo experiments showed that Ub-modifying enzymes (E1, E2s, and E3s) could not install the Ub probe onto substrate proteins prior to removal of the nitrobenzyl group, which was easily accomplished via photoirradiation. The utility and practicality of this probe were exemplified by the time-resolved biochemical and proteomic investigation of ubiquitination events in live cells during a H_2O_2-mediated oxidative stress response. This work shows a conceptually new family of chemical Ub tools for the time-resolved studies on dynamic protein ubiquitination in different biological processes and highlights the utility of modern chemical protein synthesis in obtaining custom-designed tools for biological studies.

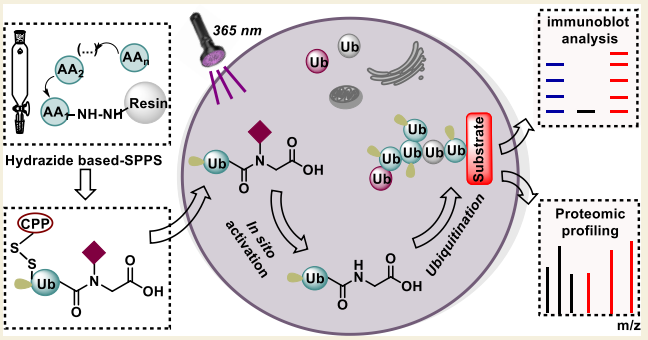

KEYWORDS: *protein ubiquitination, chemical protein synthesis, Ub probes, photocaged probes, proteomic profiling*

INTRODUCTION

Post-translational modifications of proteins greatly expand their structural and functional diversity.[1−4] As a complex post-translational modification, protein ubiquitination is orchestrated by ubiquitin (Ub)-modifying enzymes including Ub activation enzymes (E1s), conjugating enzymes (E2s), and ligases (E3s),[5] and it is antagonized by deubiquitinases (DUBs).[6] Ubiquitination on substrate proteins and its removal are highly spatiotemporal in nature,[7] and the intracellular processes they influence, such as cell cycle,[8,9] DNA damage repair,[10,11] and protein quality control,[12,13] are finely tuned. Dysregulation of ubiquitination and deubiquitination is implicated in a variety of diseases[14] including Fanconi anemia,[15,16] neurodegenerative diseases,[17] and cancers.[18]

To decipher the cellular roles of protein ubiquitination, many biochemical approaches have been developed to monitor and characterize protein ubiquitination, including the screening of ubiquitinated substrates and the determination of ubiquitination sites. Affinity-based tools such as antibodies,[19−21] antigen-binding fragments (Fabs),[22] affimers,[23] and tandem ubiquitin-binding entities (TUBEs)[24−27] enable enrichment of Ub-modified proteins. Meanwhile, the incorporation of tagged Ub into the cellular Ub pool by ectopic or stable expression allows specific affinity purification of ubiquitinated protein conjugates for global mapping of protein ubiquitination.[28−30] Despite these advances, chemical tools capable of temporal resolution probing of ubiquitination events remain to be developed.

Here, we describe the development of the first stimuli-responsive Ub probe capable of profiling intracellular changes in ubiquitination on substrates in a time-resolved manner (Scheme 1). The practicality of this tool was demonstrated by the temporal resolution probing of ubiquitination events in live cells during the H_2O_2-stimulated oxidative stress response, suggesting that the probe constitutes a conceptually new family

Received: July 28, 2023
Revised: September 16, 2023
Accepted: September 18, 2023
Published: October 3, 2023

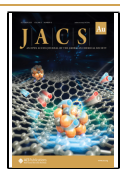

Scheme 1. Development of Stimuli-Responsive Ub Probe to Study Intracellular Dynamic Ubiquitination Processes with Temporal Resolution

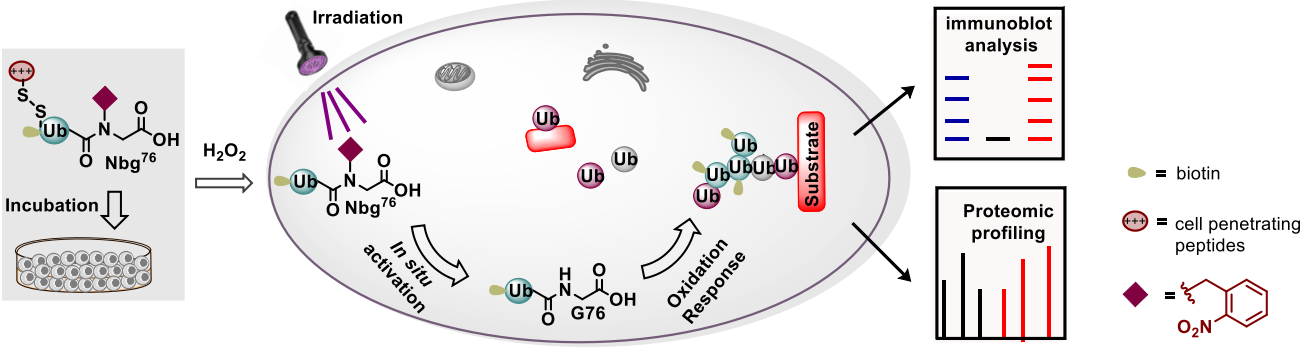

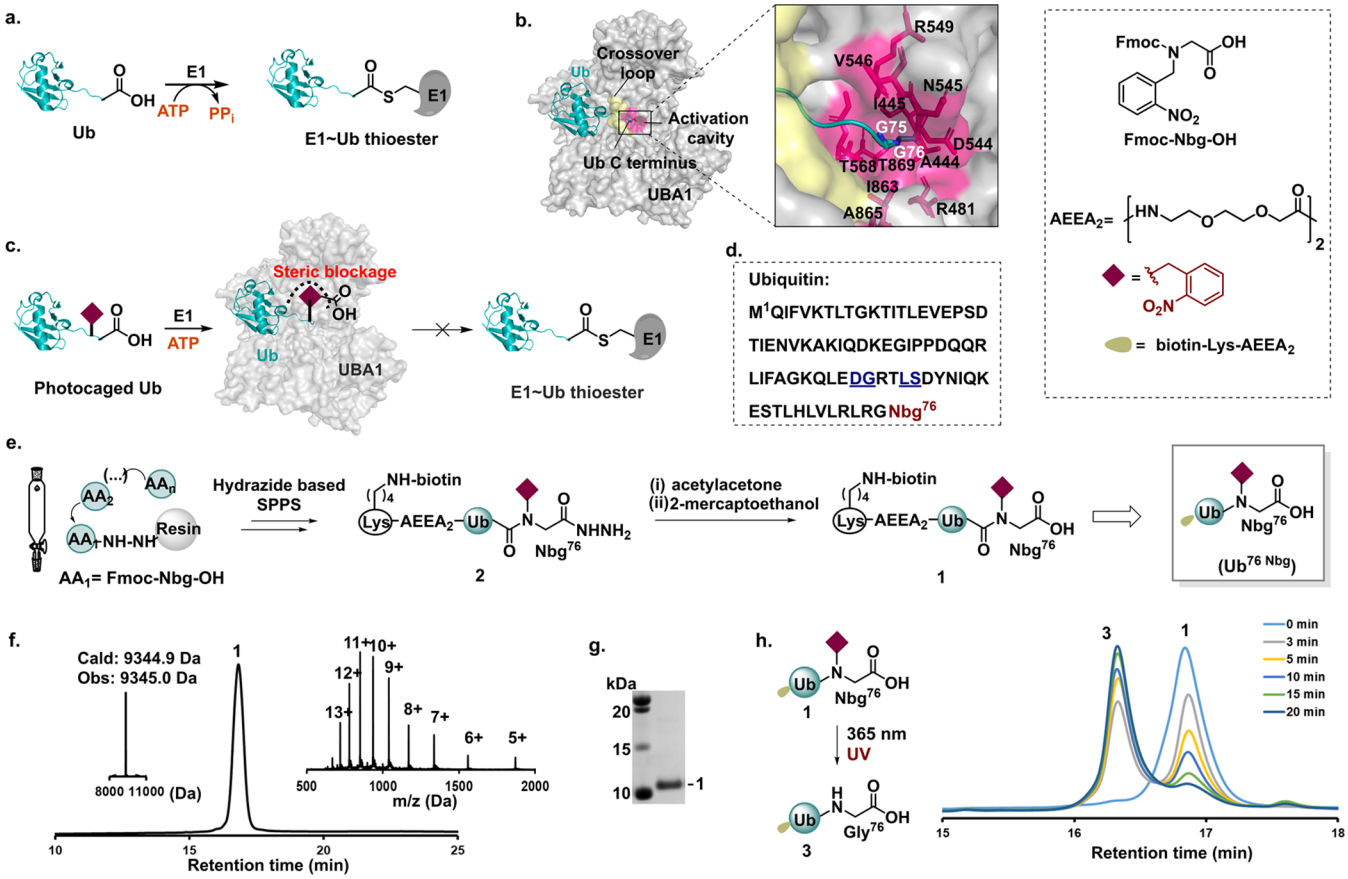

Figure 1. Chemical synthesis and characterization of the Ub probe (**1**). (a) E1 activates Ub to sequentially form Ub-AMP and E1−Ub thioester. (b) Structure of UBA1−Ub complex during Ub activation (PDB: 3CMM). Ub C terminus (Gly75, Gly76) inserts into "Ub cavity". The "Ub cavity" is colored in pink, and the "crossover loop" is colored in yellow. (c) Photocaging of Ub by installing a bulky photosensitive group at the Ub C-terminus. (d) Amino acid sequence of the synthetic Ub probe. Gly76 was replaced by Nbg, dimethoxybenzyl D^{52}-G^{53}, and pseudoproline dipeptides L^{56}−S^{57} were introduced during the synthesis to improve the yield. (e) Synthesis of **1** using hydrazine-loaded 2-Cl resin. (f) Analytical HPLC (214 nm), deconvoluted, and high-resolution ESI-MS of **1**. (g) SDS-PAGE characterization (Coomassie staining) of **1**. (h) HPLC monitoring of **1** under 365 nm photoirradiation.

of chemical tools for investigations on the dynamic coordinated processes of substrate ubiquitination in live cells.

RESULTS AND DISCUSSION

Chemical Synthesis and Characterization of the New Probe

The design of our tool is based on a key finding from a structural study of Ub-activating enzyme (UBA1),[31,32] which revealed that during Ub activation the last residue of Ub, Gly76, accepts adenosine only after passing through the crossover loop (yellow) into a narrow chamber (named "Ub cavity", colored in red) of UBA1 (Figure 1a,b). We were curious to know whether the installation of a photosensitive group at the amide bond between Ub Gly75 and Gly76 would block Ub activation (Figure 1c), the initial step of ubiquitination. To this end, we chose canonical N-(2-nitobenzyl)-Gly (Nbg) as the photocaging group,[33−39] which has been used recently in many chemical biology studies such

https://doi.org/10.1021/jacsau.3c00421
JACS Au 2023, 3, 2873−2882

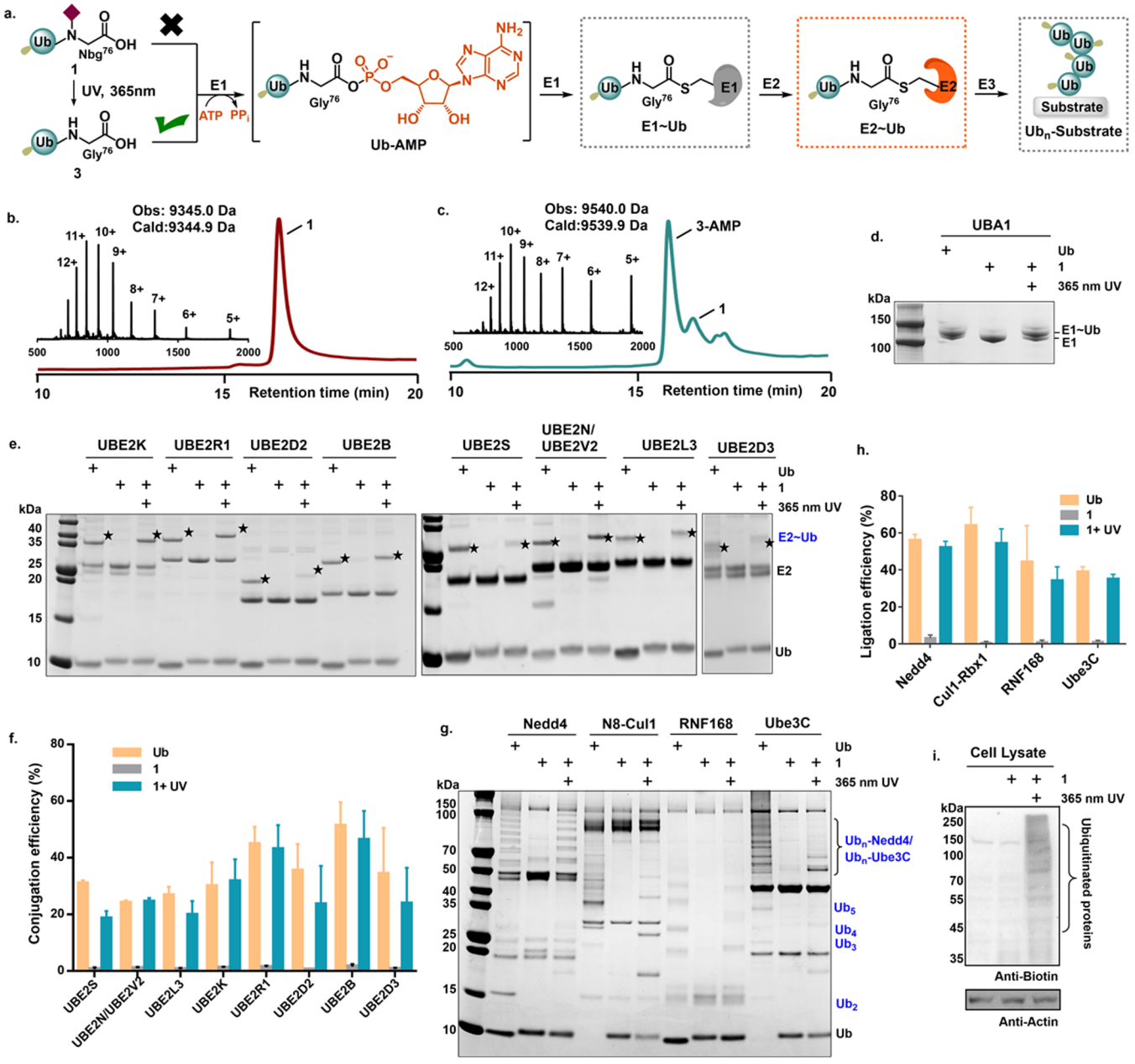

Figure 2. Ub probe (**1**) can react with E1, E2s, and E3s in vitro if exposed to photoirradiation. (a) Sequence of reactions that leads to in vitro ubiquitination, i.e., E1 activation, E2 conjugation, and E3 ligation. Wild-type Ub was used for comparison. (b) HPLC and ESI-MS analysis of adenylation by **1** via E1 enzyme UBA1. (c) HPLC and ESI-MS analysis of adenylation by **1** via E1 enzyme UBA1 with irradiation. (d) SDS-PAGE analysis (Coomassie staining) of photo-dependent activation of **1** by UBA1 to form a thioester adduct. (e) SDS-PAGE analysis (Coomassie staining) of conjugation of **1** by E2s. The star represents the E2-Ub thioester conjugate. (f) Quantitation of the conjugation efficacy. The conjugation efficacy was calculated by (band intensity of E2 − Ub conjugate)/(band intensity of E2 − Ub conjugate + band intensity of E2). Data were plotted as mean ± SEM of three independent biological replicates. (g) SDS-PAGE analysis (Coomassie staining) of ligation of **1** by E3s to substrate proteins. (h) Quantitation of the ligation efficacy. The ligation efficacy was calculated similar to that in Figure 2f. Data were plotted as mean ± SEM of three independent biological replicates. (i) Immunoblotting analysis of utilization of **1** by Ub-modifying enzymes in cell lysate using anti-biotin antibody.

as control of protein activity[40,41] and PROTAC-induced protein degradation.[42]

We used microwave-assisted solid-phase peptide synthesis (SPPS) to make Nbg-modified Ub, i.e., Ub probe (**1**), which also incorporated biotin on the N-terminal for immunoblotting (Figure 1d). Unfortunately, the use of Wang resin gave only the truncated byproduct Ub(1−74)-COOH, perhaps due to the bulky group on the backbone amide of Gly75-Gly76, triggering the formation of diketopiperazines (DKP) (Scheme S1).[43,44] However, using hydrazine-loaded 2-Cl trityl resin, which recently enabled the synthesis of challenging peptides, each bearing a C-terminal carboxylate,[45] Ub^{76Nbg}-$NHNH_2$ (**2**) was expediently synthesized without any observable DKP formation (Figures 1e and S1a−c). Conversion of Ub^{76Nbg}-$NHNH_2$ into **1** was accomplished using acetylacetone and *β*-mercaptoethanol without prepurification (Figures 1e and S1d,e). The identity and purity of **1** were confirmed by high-performance liquid chromatography (HPLC), electrospray

https://doi.org/10.1021/jacsau.3c00421
JACS Au 2023, 3, 2873−2882

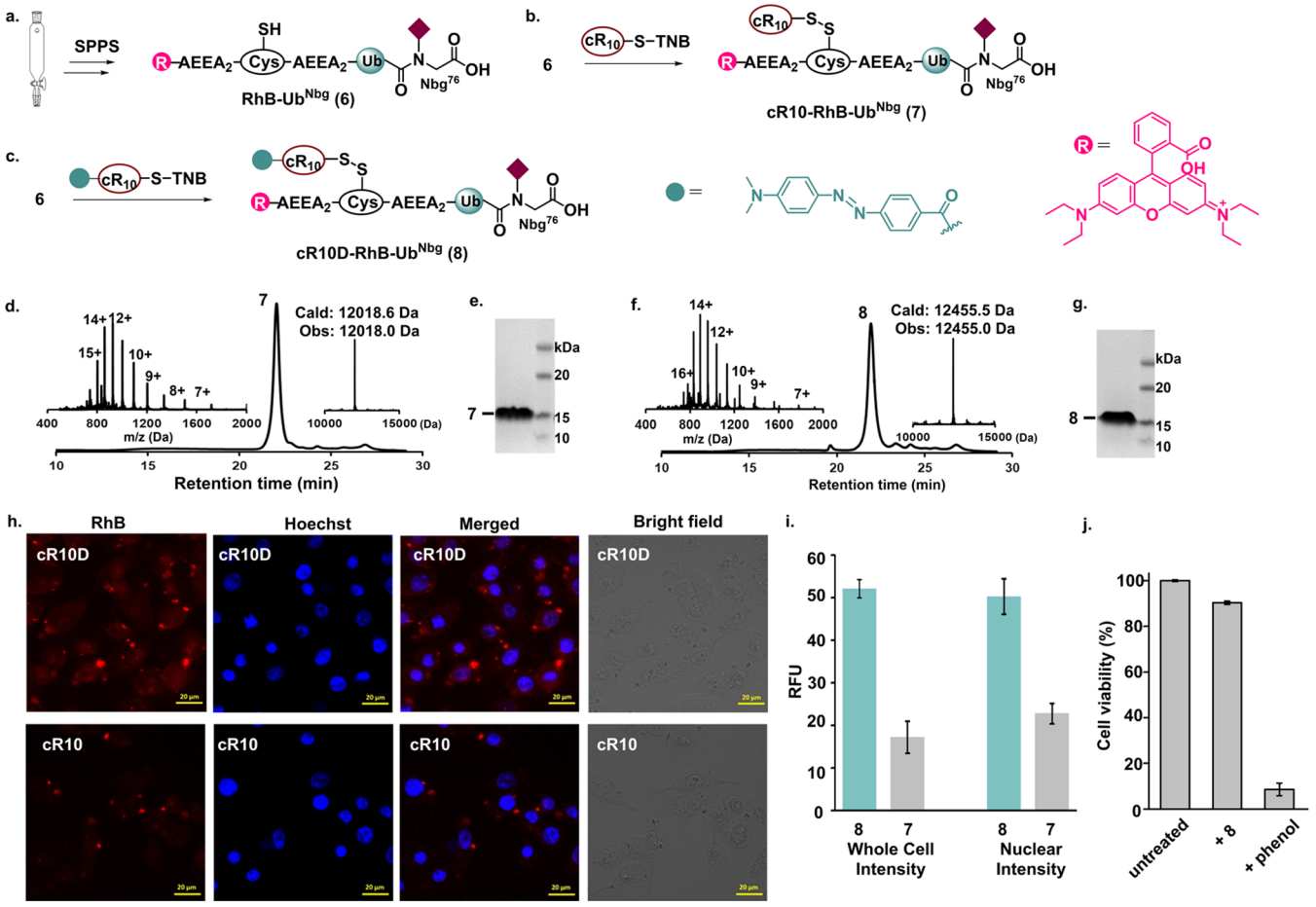

Figure 3. Delivery of a stimuli-responsive Ub probe into live cells. (a) Chemical synthesis of RhB-Ub^{Nbg} (**6**). (b, c) Synthesis of cell-permeable photocaged Ub probes **7** and **8**. (d–g) Analytical HPLC (214 nm), deconvoluted and high-resolution ESI-MS, and SDS-PAGE characterization (Coomassie staining) of **7** and **8**. (h) Living cell fluorescence imaging of HeLa cells treated with 5 μM **7** and **8**. **7** and **8** were visualized by TER fluorescence (red channel), and Hoechst was used for nuclear staining (blue channel). (i) Quantification of whole cell and nuclear RhB intensity of the cell images after delivery of **7** and **8**. Data were plotted as mean ± SEM of three independent biological replicates. (j) MTT assay analysis of cell viability treated with 5 μM **8** for 1 h. Treatment with 0.64% phenol was used as a positive control. Data were plotted as mean ± SEM of three independent biological replicates.

ionization mass spectrometry (ESI-MS), and sodium dodecyl sulfate polyacrylamide gel electrophoresis (SDS-PAGE) (Figure 1f,g). About 25 mg of purified **1** was obtained from 0.125 mmol of resin, for an overall isolated yield of 2.5%.

Next, we examined whether the photosensitive group in **1** could be removed by photoirradiation. To this end, **1** was irradiated with 365 nm UV light (10 mW/cm^2) for 3, 5, 10, 15, and 20 min, and the reaction was monitored by HPLC coupled with ESI-MS. After 3 min, a new peak corresponding to a product with a molecular weight of 9210.0 Da was observed (Figures 1h and S2), consistent with the formation of decaged product **3**. The decaging yield gradually increased with an increasing irradiation time, from approximately 50% at 3 min to a maximum of 90% (quantified by HPLC) at 20 min. These results demonstrate that the caging group in **1** can be readily removed to produce wild-type Ub by 365 nm UV light.

Ub Probe (1) Cannot React with E1, E2s, and E3s In Vitro without Photoirradiation

With **1** in hand, we examined its activity in in vitro ubiquitination reactions (Figure 2a). First, **1** (40 μM) was incubated with E1 UBA1 (20 μM) in HEPES buffer (pH 7.5) containing 10 mM ATP, and the reaction was monitored by HPLC coupled with ESI-MS. Without photoirradiation, only one peak at 9345.0 Da corresponding to unreacted **1** was detected, even after the incubation time was extended to 60 min (Figures 2b and S3a). This shows that **1** is inert under the reaction conditions in the absence of photoirradiation. In contrast, when the reaction was photoirradiated for 15 min, we were pleased to find a major peak at 9540.0 Da corresponding to the adduct of decaged product **3** with adenosine 5′-monophosphate (AMP), i.e., **3**-AMP, suggesting that **1** can be effectively adenylated by UBA1 after irradiation (Figures 2c and S3b,c). SDS-PAGE analysis of the activation reaction revealed that although almost no new adduct band was detected after 20 min of incubation in the absence of irradiation, a band with a molecular weight of UBA1-Ub adduct was formed upon irradiation of the reaction, further demonstrating that **1** can only be activated by UBA1 after photoirradiation (Figure 2d).

The conjugation of **1** by E2s was examined using both Ub chain-specific E2s (including UBE2S, UBE2K, UBE2R1, and UBE2N/UBE2V2) and nonspecific E2s (including UBE2B, UBE2D2, UBE2D3, and UBE2L3).[46] Probe **1** (40 μM) was incubated with E1 (0.5 μM) and one of the aforementioned E2s (5 μM) in HEPES buffer (pH 7.5) for 15 min; the reaction was analyzed by SDS-PAGE. Once again, almost no product

https://doi.org/10.1021/jacsau.3c00421
JACS Au 2023, 3, 2873−2882

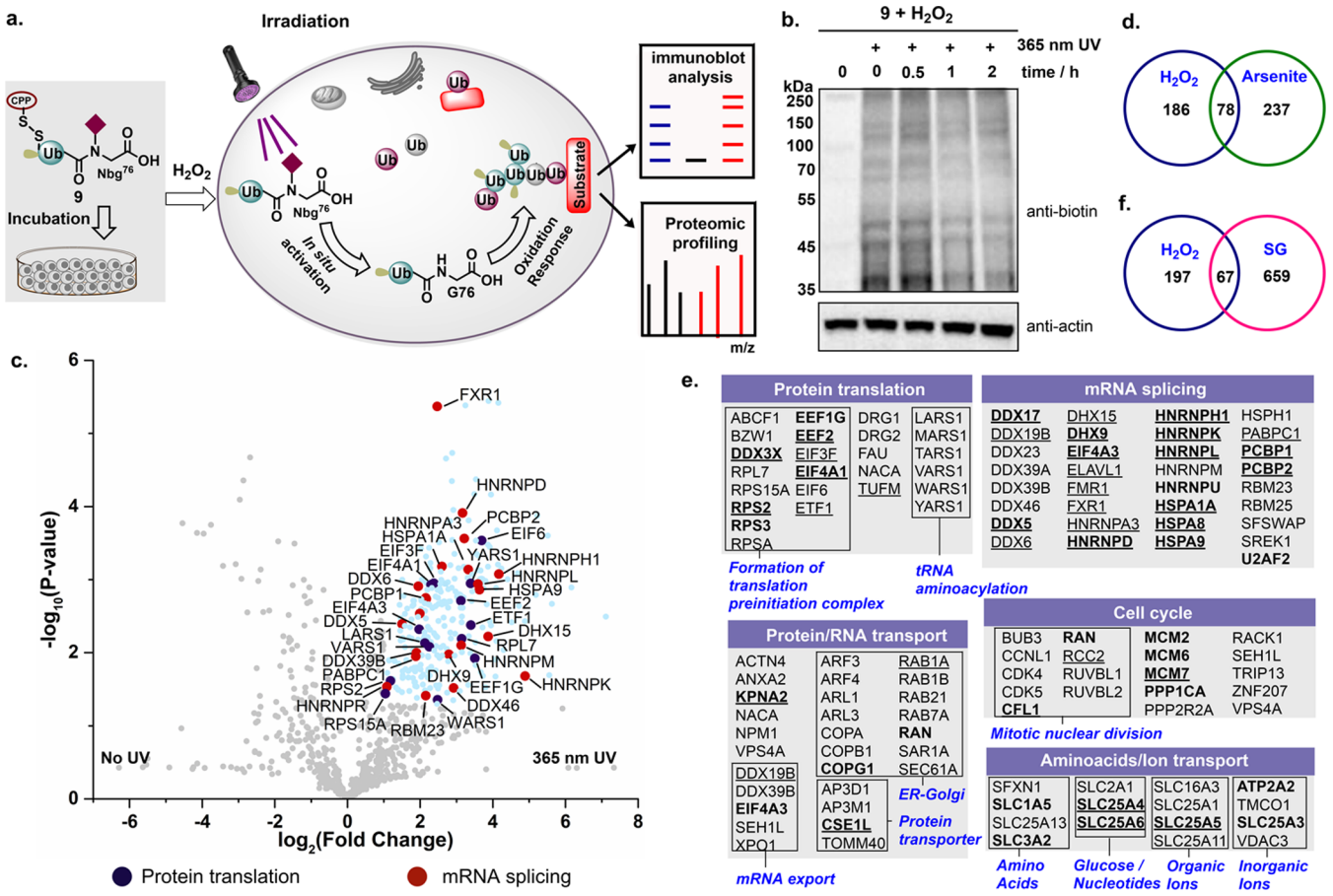

Figure 4. Time-resolved probing of newly occurred ubiquitination events using cell-permeable Ub probe (**9**) under H_2O_2-mediated oxidative stress. (a) Schematic presentation of the investigation of newly occurred ubiquitination events using **9**. (b) Immunoblotting analysis of the protein ubiquitination level at different times after H_2O_2 treatment using **9**. (c) Volcano plot of pairwise comparison proteins captured by **9** with/without photoirradiation. Significantly enriched proteins are colored cyan. (d) Venn diagram of proteins captured by **9** under H_2O_2-mediated oxidative stress and captured by TUBEs under arsenite-mediated oxidative stress. (e) DAVID functional clustering of biological pathways targeted by enriched proteins. Bold: proteins that were also enriched in arsenite-mediated oxidative stress; underline: proteins that were also identified as components of stress granules. (f) Venn diagram of proteins captured by **9** under H_2O_2-mediated oxidative stress and proteins reported to be the components of stress granules.

band corresponding to the conjugated product was detected for any of E2s. Only after the reaction was irradiated for 15 min could the expected E2-Ub conjugation bands be seen (Figure 2e). To assess the conjugation efficiency of **1** by E2 after photoirradiation, we calculated the (band intensity of E2 − Ub conjugate)/(band intensity of E2 − Ub conjugate + band intensity of E2), which showed that the efficiency was comparable with the wild-type Ub by UBE2B, UBE2K, UBE2L3, UBE2N, and UBE2R1 and slightly lower than wild-type Ub by UBE2D2, UBE2D3, and UBE2S (Figure 2f).

Next, we examined the activity of **1** toward an E3-mediated Ub ligation involving the RING (really interesting new gene) family E3s, Cullin-Rbx1 and RNF168, and the HECT (homologous to the E6AP carboxyl terminus) family E3s, UBE3C and Nedd4.[47] Probe **1** was incubated with E1 (0.5 μM), E2 (5 μM), and E3 (1 μM) in HEPES buffer (pH 7.5) for 30 min. SDS-PAGE analysis revealed that **1** was largely inert until irradiation, after which it was effectively ligated by the E3s to generate either free Ub chains (for RING-type E3s) or ubiquitinated substrates (ubiquitinated E3s for HECT family E3s) (Figure 2g). We also quantitatively evaluated the ligation efficiency of **1** by E3 after photoirradiation, which revealed that the efficiency was comparable with wild-type Ub (Figure 2h). Finally, we tested the utilization of **1** in a more complex biological environment containing various Ub-modifying enzymes. Then, probe **1** was incubated for 15 min in HeLa cell lysate which was then analyzed by immunoblotting with an antibiotin antibody. The obvious band corresponding to Ub-modified substrates appeared only after photoirradiation of the cell lysate (Figure 2i).

It should be noted that Ub^{75Nbg} (**5**) bearing an Nbg group at the backbone amide of Arg74-Gly75 can also be readily synthesized and efficiently converted to **3** after photoirradiation (Figure S4). In vitro ubiquitination reaction revealed that, like **1**, **5** can only be activated by UBA1 and conjugated by E2s after photoirradiation (Figure S5). Collectively, the above results suggested that the stimuli-responsive Ub probe can be attached to the substrate proteins by E1, E2s, and E3s in a photoirradiation-controlled manner.

Delivery of Ub Probe into Live Cells Using Cell-Penetrating Peptides

We next investigated the delivery of stimuli-responsive Ub probe into live cells to examine whether it could be conjugated by endogenous E1, E2s, and E3s in a photoinduced manner. Our strategy to accomplish the cellular delivery was based on the recently developed cell-penetrating peptide (CPP) cyclic

https://doi.org/10.1021/jacsau.3c00421
JACS Au 2023, 3, 2873−2882

deca-arginine (cR10) and 4-((4-(dimethylamino)phenyl)azo)-benzoic acid (DABCYL)-modified cR10, cR10DABCYL (cR10D).[48−51] cR10 and cR10D containing a cysteine were prepared and activated using 5, 5′-dithion-bis-2-nitrobenzoic acid (DTNB) (Figures S6 and S7). Rhodamine B (RhB)-labeled Ub^{Nbg} (**6**), synthesized by appending cysteine and RhB to the N-terminal of Ub (Figures 3a and S8), where the RhB label serves as a fluorophore for intracellular imaging, was reacted with DTNB-activated cR10 (Figure 3b) or cR10D (Figure 3c) in 6 M GnHCl to give cR10-RhB-Ub^{Nbg} (**7**) (in 45% isolated yield) and cR10D-RhB-Ub^{Nbg} (**8**) (in 40% isolated yield), respectively (Figures 3d−g, S9, and S10).

With fluorescently labeled CPP-Ub conjugates **7** and **8** in hand, we tested their cellular uptake. HeLa cells were separately incubated with a medium containing **7** and **8** (5 μM) at 37 °C for 1 h, washed with phosphate buffer saline (PBS), and stained with the Hoechst nuclei dye. The cell permeability of **7** and **8** was analyzed by confocal laser scanning microscopy (CLSM), which showed that the cytosol and nuclei of cells treated with **8** exhibited a higher intensity of red fluorescence compared with those treated with **7** (Figures 3h and S11), indicating that **8** was more efficiently delivered into the cells. We further quantified the absolute RhB intensity of **7** and **8** in over 200 whole cells and their nuclei. Our results showed that the fluorescence intensity of **8** increased about twofold compared to that of **7** (Figure 3i), confirming that cR10D improved the cellular uptake of Ub probe, consistent with the reported results.[50] We also found that the morphology of Hoechst-stained nuclei was normal, suggesting that the cellular uptake of **8** does not cause significant toxicity. The effect of **8** on cell proliferation was measured using the MTT assay, which showed that the treatment of **8** at 5 μM had a minimal effect on cell viability (Figure 3j)

Time-Resolved Probing of Ubiquitination in Live Cells Using Cell-Permeable Ub Probe

We next assessed whether stimuli-responsive Ub probes can be installed onto substrate proteins, activated by irradiation, and thereafter used to probe the proteome-wide dynamic cellular ubiquitination processes under different conditions (Figure 4a). For this purpose, we synthesized a cell-permeable cR10D-biotin-Ub^{Nbg} (**9**) for the proteomic profiling of newly ubiquitinated proteins by immunoblotting or enrichment (Figures S12 and S13). Compound (**9**) was similar to cR10D-RhB-Ub^{Nbg} (**8**), where RhB was replaced with biotin for enrichment. After cellular incubation of **9** (5 μM) at 37 °C for 1 h, cells were irradiated with 365 nm light (10 mW/cm^2), then stimulated with 1 mM H_2O_2 for 15 min, and subsequently cultured in a medium without H_2O_2 (recovery) for 0, 30, 60, and 120 min, respectively. The cells were lysed and analyzed with immunoblotting using anti-biotin antibody.

Almost no bands were observed in lanes of the nonirradiated sample, whereas the UV-treated samples displayed significant biotinylated protein bands (i.e., ubiquitinated proteins) from low to high molecular regions (Figure 4b). These results suggested that **9** could not react with Ub-modifying enzymes unless first exposed to photo-irradiation, after which it could be activated and attached to cellular substrate proteins. We further found that the intensity of the band corresponding to ubiquitinated proteins first increased within 30 min and then began to decrease (Figure 4b), indicating that the level of global protein ubiquitination rose upon exposure to H_2O_2, which might be required for the clearance of damaged/misfolded proteins by proteasome,[52] and then returned to baseline within 2 h during the recovery phase in fresh medium. The dynamic fluctuations of global ubiquitination level in response to oxidative stress were also demonstrated in recent studies using an anti-Ub antibody.[53] Collectively, these experiments indicated that **9** can be photoactivated on demand and used to monitor the dynamic processes of ubiquitination in live cells in a time-resolved manner.

Next, we sought to identify the proteins ubiquitinated during H_2O_2-mediated oxidative stress response, via the intracellular proteome-wide profiling of HeLa cells using **9**. HeLa cells were incubated with **9** (5 μM) for 1 h, irradiated with 365 nm light (10 mW/cm^2) for 15 min, and then treated with 1 mM H_2O_2 and cultured for 30 min; cells without irradiation were used as a control. Each assay was replicated three times. Cells were collected and lysed, and the ubiquitinated proteins were enriched by streptavidin beads, separated by SDS-PAGE, and analyzed by label-free quantitative (LFQ) mass spectrometry. A volcano plot was generated by plotting -$\log_{10}$(P-value) against the fold enrichment ([$\log_2$(+UV/−UV)]) of the LFQ intensities of the paired samples (Figure 4c). With a threshold of [$\log_2$(+UV/−UV)]>1 (twofold enrichment), -$\log_{10}$(p Value)>1.3 (p Value <0.05), a total of 264 proteins were found to be significantly enriched (colored cyan, Figure 4c). Our results showed that the number of proteins (264) enriched by **9** was comparable to the reported number of ubiquitinated substrates (315) captured by TUBEs under arsenite-mediated oxidative stress.[54] The enriched proteins captured with **9** included 78 proteins, also identified by TUBEs to be ubiquitinated under arsenite-mediated oxidative stress, including proteins involved in translation initiation (EEF1G, EEF2, and EIF4A1), mRNA splicing (DDX17, HNRNPD, HNRNPK, HNRNPL, PCBP1, and PCBP2), and DNA replication (MCM2, MCM6, and MCM7), indicating that ubiquitination might regulate these processes during the oxidative stress response (Figures 4d and S14). Gene ontology (GO) analysis using the DAVID bioinformatics resources[55] revealed that 264 enriched proteins are involved in protein translation, mRNA splicing, RNA/protein transport, ion transport, cell cycle, cytoskeleton, and metabolism (Figures 4e and S15). Additionally, 67 enriched proteins were reported to be stress granule (SG) proteins (Figures 4f and S16),[54] including the components of translation preinitiation complex (EEF2, EIF3F, EIF4A1, and ETF1), RNA helicases (DDX17, DDX19B, DDX5, DDX6, DHX15, and DHX9), heterogeneous nuclear ribonucleoproteins (HNRNPA3, HNRNPD, HNRNPH1, HNRNPK, and HNRNPL), and mRNA-binding protein PABPC1 (Figure 4e). This is consistent with a recent finding that stress granule-associated Ub chains are primarily conjugated with substrates,[56] suggesting the participation of ubiquitination in the assembly of stress granules under oxidative stress. Notably, the enriched proteins also include 15 mitochondrial proteins implicated in the transport of amino acids, nucleotides, and ions, suggesting that ubiquitination might also play a role in regulating mitochondrial homeostasis under H_2O_2-stimulated oxidative stress. Taken together, these results indicate that our stimuli-responsive Ub probe can be used with proteomic identification tools to better understand the conditional ubiquitination of proteins in different biological contexts.

https://doi.org/10.1021/jacsau.3c00421
JACS Au 2023, 3, 2873−2882

CONCLUSIONS

A cell-permeable stimuli-responsive Ub probe capable of a time-resolved study of substrate ubiquitination in live cells has been developed. The design of our probe is based on the insight that the installation of a photolabile group (e.g., Nbg) on the C-terminal of Ub can effectively impede the attachment of Ub to substrate proteins by Ub-modifying enzymes. Using our probe, along with the state-of-the-art cell-penetrating peptide cR10D, we were able to carry out a time-resolved study of ubiquitination events under different cellular processes, as exemplified by H_2O_2-mediated oxidative stress response in this work. Because our Ub probe can be activated on demand, it enables the direct profiling of newly occurring ubiquitination events in the presence of existing Ub-modified proteins under different biological contexts when combined with modern proteomic technologies. In contrast, conventional biological methods such as TUBEs capture both pre-existing and newly Ub-modified proteins in a single profiling workflow, so that they require examination of Ub modifications in the presence and absence of the indicated stress separately, which may complicate the identification of newly occurring ubiquitination processes.

Taken together, our results establish a conceptually new family of chemical tools for time-resolved studies on protein ubiquitination in live cells and further exemplify the utility of chemically synthesized customized probes that are more readily synthesizable and are of different structural designs for the study of Ub modifications.[57−66] It should be mentioned that although the current photocaging group, Nbg, requires 365 nm of UV light and may cause cytotoxicity in some experiments, our probe can be easily extended to use more benign photosensitive groups[67] that would meet the requirements for specific biological conditions.

METHODS

Fmoc-Based Peptide Synthesis

All peptides or proteins in this work were obtained from the 9-fluorenyl-methoxycarbonyl (Fmoc)-based solid-phase peptide synthesis (SPPS). For manual Fmoc-SPPS, both coupling and deprotection were performed at 35 °C. The coupling reactions were performed with 4.0 equiv of amino acids, 4.0 equiv of HCTU, and 8.0 equiv of DIEA in DMF solution for 30 min. The deprotection reactions were performed with 20% (v/v) piperidine in a DMF solution for 10 min. For automatic Fmoc-SPPS, the synthesis was conducted on an automated microwave peptide synthesizer (Liberty BlueTM, CEM Corp., U.S.A.). Typically, peptide or protein synthesis began with the resin swelling in DMF for 5−10 min. Each coupling cycle includes Fmoc deprotection using 20% piperidine (containing 0.1 M Oxyma) in DMF (1 min at 90 °C) and amino acid coupling using protected amino acids (4 equiv), DIC (8 equiv), and Oxyma (4 equiv) in DMF (10 min at 50 °C for His and Cys and 1.5 min at 89 °C for other residues). After every reaction, DMF was added to wash the resin three times. After the completion of the synthesis, the resin was washed with DMF, DCM three times, and dried over a high vacuum. Twenty milliliters of the cleavage reagent (TFA: phenol: H_2O: thioanisole: 1,2-ethanedithiol (EDT) = 82.5:5:5:5:2.5) was then added to the resin and shaken for 2.5 h at 37 °C to cleave the peptides from the resin. The resin was filtered, and the combined filtrate was blown to about 6 mL by nitrogen bubbling; then, 40 mL of cold ether was added to the filtrate to precipitate the crude peptide. Finally, the crude peptide was washed with 40 mL of cold ether for two times.

In Vitro Photodecaging Assay

To examine the decaging efficiency of **1** under photoirradiation, 100 μM folded **1** (∼1 mg/mL in PBS 7.4) was irradiated using a photo-cross-linker (Scientz, Ningbo) with 365 nm UV for 3, 5, 10, 15, and 20 min, and the reaction was monitored by HPLC and analyzed with ESI-MS.

In Vitro Ubiquitination Assay

In the E1 activating assay, for HPLC analysis of the activating reaction, 20 μM HUBA1 and 40 μM **1** were mixed in buffer containing 50 mM HEPES, pH 7.5, 10 mM ATP, and 10 mM $MgCl_2$. The reaction was incubated for indicated times with/without photoirradiation (for 15 min). The reaction was analyzed by RP-HPLC coupled with ESI-MS. For SDS-PAGE analysis of the ubiquitin activation process, 1 μM HUBA1 and 10 μM of **1** or **5** were mixed in buffer containing 50 mM HEPES, pH 7.5, 10 mM ATP, and 10 mM $MgCl_2$. The reaction was incubated for indicated times with/without photoirradiation. The reaction was stopped by the addition of an equal volume of LDS loading buffer and analyzed by SDS-PAGE.

For Ub conjugating assay, 0.5 μM E1, 5 μM E2, and 40 μM **1** or **5** were mixed in buffer containing 50 mM HEPES, pH 7.5, 10 mM ATP, and 10 mM $MgCl_2$. The reaction was incubated for 15 min with/without photoirradiation (for 15 min). The reaction was stopped by the addition of equal volume of LDS loading buffer and analyzed by SDS-PAGE.

For the Ub ligating assay, 0.5 μM E1, 5 μM E2, 1 μM E3, and 40 μM of **1** were mixed in buffer containing 50 mM HEPES, pH 7.5, 10 mM ATP, and 10 mM $MgCl_2$. The reaction was incubated for 30 min with/without photoirradiation (for 15 min). The reaction was stopped by the addition of equal volume of LDS loading buffer and analyzed by SDS-PAGE.

For the cell lysate-based ubiquitination assay, 40 μM of **1** was added into the HeLa cell lysate. The reaction was incubated for 30 min with/without photoirradiation (for 15 min). The reaction was stopped by the addition of equal volume of LDS loading buffer and analyzed by immunoblotting using anti-biotin antibody.

Protein Cell Delivery, Confocal Microscopy, and Image Analysis

HeLa cells were plated onto sterile 35 mm glass-bottom dishes (biosharp BS-20-GJM) for 24 h at 37 °C and 5% CO_2 in DMEM (Gibco C11965500BT) supplemented with 10% FBS (Lonsera S711−001S), 100 units/mL penicillin, and 0.1 mg/mL streptomycin (HyClone SV30010); then, cells were treated with fresh DMEM (no phenol red, Gibco 21063029) containing 5 μM of **7** or **8**, respectively, at 37 °C. After 1 h, cells were washed with cold phosphate-buffered saline (PBS) solution with calcium and magnesium (Hyclone SH30256.01) three times and then stained with the dye Hoechst 33258 according to the manufacturer's instructions for live cell imaging.

The cells were imaged using an argon laser (405 nm) and argon laser (543 nm) for visualizing Hoechst 33258 (blue nuclear staining) and RhoB (red emission), respectively, with a Plan-Apochromat 63X/1.4 Oil DIC M27 lens on a Zeiss LSM 880 AxioObserver confocal laser scanning microscope. All treatments were performed in three separate experiments.

Images were analyzed by using FiJi software. Quantification of the percentage of cells having cytosol-delivered probes was achieved by calculating the total number of cells and the number of cells having the RhB signal. The absolute RhB intensity inside the nucleus was clarified using a cell-masking algorithm based on Hoechst 33258.

Immunoblotting Analysis of the Protein Ubiquitination Level at Different Times after H_2O_2 Treatment

HeLa cells were treated with 5 μM of **9** for 1 h at 37 °C; then, the cells were washed with cold PBS. Subsequently, HeLa cells were irradiated with 365 nm UV light for 15 min in PBS buffer or without UV treatment, followed by incubation with DMEM containing 1 mM H_2O_2 for 15 min. Then, the cells were incubated with fresh DMEM for 0.5, 1, and 2 h, respectively. HeLa cells were lysed at a specific time point with RIPA lysis buffer containing 1 mM 2-iodoacetamide and allowed to incubate on ice for 30 min and then centrifuged at 11,000 rpm at 4 °C for 10 min to remove cell debris. Total protein concentration was determined using a Bradford assay (Sangon

https://doi.org/10.1021/jacsau.3c00421
JACS Au 2023, 3, 2873−2882

Biotech). 100 μg cell lysates were used immediately for immunoblotting using an antibiotin antibody.

Pulldown and Mass Spectrometry Analysis

For intracellular proteome-wide protein profiling using label-free quantitative (LFQ) mass spectrometry analysis, the cell lysate generated from **9** and H_2O_2-treated HeLa cells, as described above, was incubated with streptavidin agarose beads (Promega) at 4 °C for 2 h. Next, the beads were washed sequentially with 1 × binding buffer (25 mM tris,150 mM NaCl, 1 mM DTT, 0.5% v/v NP-40, pH 7.6), 2 × of 0.5% SDS in PBS, 2 × 1 M NaCl in PBS, 2 × Tris-buffered saline, and 10 × 50 mM NH_4HCO_3 at pH 8.0. The enriched proteins were eluted from beads with LDS loading buffer at 95 °C for 10 min. Then, the samples were resolved by SDS-PAGE and analyzed by LFQ mass spectrometry. Each pulldown experiment was performed in three replicates. LC-MS/MS analysis was conducted as described previously.[68]

■ ASSOCIATED CONTENT

Supporting Information

The Supporting Information is available free of charge at https://pubs.acs.org/doi/10.1021/jacsau.3c00421.

Routine reagents and instruments, experimental procedures (including protein expression and purification, synthesis and characterization of peptides and probes, in vitro and in vivo ubiquitination assay, protein refolding, delivery of probes into live cells, and pulldown and mass spectrometry analysis), and experimental results (PDF)

Proteomic data of ubiquitinated proteins (XLSX)

■ AUTHOR INFORMATION

Corresponding Authors

Lei Liu − *Tsinghua-Peking Center for Life Sciences, Ministry of Education Key Laboratory of Bioorganic Phosphorus Chemistry and Chemical Biology, Center for Synthetic and Systems Biology, Department of Chemistry, Tsinghua University, Beijing 100084, China; Center for BioAnalytical Chemistry, Hefei National Laboratory of Physical Science at Microscale, University of Science and Technology of China, Hefei 230026, China;* orcid.org/0000-0001-6290-8602; Email: lliu@mail.tsinghua.edu.cn

Yi-Ming Li − *School of Food and Biological Engineering, Engineering Research Center of Bio-process, Ministry of Education, Hefei University of Technology, Hefei 230009, China;* orcid.org/0000-0002-2161-2482; Email: ymli@hfut.edu.cn

Authors

Lu-Jun Liang − *Tsinghua-Peking Center for Life Sciences, Ministry of Education Key Laboratory of Bioorganic Phosphorus Chemistry and Chemical Biology, Center for Synthetic and Systems Biology, Department of Chemistry, Tsinghua University, Beijing 100084, China; Center for BioAnalytical Chemistry, Hefei National Laboratory of Physical Science at Microscale, University of Science and Technology of China, Hefei 230026, China*

Yu Wang − *School of Food and Biological Engineering, Engineering Research Center of Bio-process, Ministry of Education, Hefei University of Technology, Hefei 230009, China*

Xiao Hua − *Department of Chemistry, University of Science and Technology of China, Hefei 230026, China*

Rujing Yuan − *School of Food and Biological Engineering, Engineering Research Center of Bio-process, Ministry of Education, Hefei University of Technology, Hefei 230009, China*

Qiong Xia − *School of Food and Biological Engineering, Engineering Research Center of Bio-process, Ministry of Education, Hefei University of Technology, Hefei 230009, China*

Rongtian Wang − *School of Food and Biological Engineering, Engineering Research Center of Bio-process, Ministry of Education, Hefei University of Technology, Hefei 230009, China*

Chuntong Li − *Tsinghua-Peking Center for Life Sciences, Ministry of Education Key Laboratory of Bioorganic Phosphorus Chemistry and Chemical Biology, Center for Synthetic and Systems Biology, Department of Chemistry, Tsinghua University, Beijing 100084, China; Center for BioAnalytical Chemistry, Hefei National Laboratory of Physical Science at Microscale, University of Science and Technology of China, Hefei 230026, China*

Guo-Chao Chu − *School of Food and Biological Engineering, Engineering Research Center of Bio-process, Ministry of Education, Hefei University of Technology, Hefei 230009, China; Tsinghua-Peking Center for Life Sciences, Ministry of Education Key Laboratory of Bioorganic Phosphorus Chemistry and Chemical Biology, Center for Synthetic and Systems Biology, Department of Chemistry, Tsinghua University, Beijing 100084, China*

Complete contact information is available at: https://pubs.acs.org/10.1021/jacsau.3c00421

Author Contributions

⊥L.-J.L., Y.W., and X.H. contributed equally.

Notes

The authors declare no competing financial interest.

■ ACKNOWLEDGMENTS

This study was supported by the National Key R&D Program of China (No. 2022YFC3401500), NSFC (Nos. 22277020, 22227810, 22137005, and 92253302), the Science and Technological Fund of Anhui Province for Outstanding Youth (No. 2208085J42), and the China Postdoctoral Science Foundation (2021M691747 for G.-C.C. and 2021M701862 and 2022T150347 for L.-J.L.). The work is also supported by Vanke Special Fund for Public Health and Health Discipline Development, Tsinghua University (No. 2022Z82WKJ014) and Beijing Life Science Academy (No. 2023000CC0130). The authors thank the protein chemistry facility at the Center for Biomedical Analysis of Tsinghua University for sample analysis.

■ REFERENCES

(1) Deribe, Y. L.; Pawson, T.; Dikic, I. Post-translational modifications in signal integration. *Nat. Struct. Mol. Biol.* **2010**, *17*, 666−672.

(2) Wright, T. H.; Bower, B. J.; Chalker, J. M.; Bernardes, G. J.; Wiewiora, R.; Ng, W.-L.; Raj, R.; Faulkner, S.; Vallée, M. R. J.; Phanumartwiwath, A.; Coleman, O. D.; Thézénas, M.; Khan, M.; Galan, S. R. G.; Lercher, L.; Schombs, M. W.; Gerstberger, S.; Palm-Espling, M. E.; Baldwin, A. J.; Kessler, B. M.; Claridge, T. D. W.; Mohammed, S.; Davis, B. G. Posttranslational mutagenesis: A chemical strategy for exploring protein side-chain diversity. *Science* **2016**, *354*, No. aag1465.

(3) Josephson, B.; Fehl, C.; Isenegger, P. G.; Nadal, S.; Wright, T. H.; Poh, A. W.; Bower, B. J.; Giltrap, A. M.; Chen, L.; Batchelor-

McAuley, C.; Roper, G.; Arisa, O.; Sap, J. B. I.; Kawamura, A.; Baldwin, A. J.; Mohammed, S.; Compton, R. G.; Gouverneur, V.; Davis, B. G. Light-driven post-translational installation of reactive protein side chains. *Nature* **2020**, *585*, 530−537.
(4) Mollner, T. A.; Isenegger, P. G.; Josephson, B.; Buchanan, C.; Lercher, L.; Oehlrich, D.; Hansen, D. F.; Mohammed, S.; Baldwin, A. J.; Gouverneur, V.; Davis, B. G. Post-translational insertion of boron in proteins to probe and modulate function. *Nat. Chem. Biol.* **2021**, *17*, 1245−1261.
(5) Komander, D.; Rape, M. The ubiquitin code. *Annu. Rev. Biochem.* **2012**, *81*, 203−229.
(6) Clague, M. J.; Urbé, S.; Komander, D. Breaking the chains: deubiquitylating enzyme specificity begets function. *Nat. Rev. Mol. Cell Biol.* **2019**, *20*, 338−352.
(7) Grabbe, C.; Husnjak, K.; Dikic, I. The spatial and temporal organization of ubiquitin networks. *Nat. Rev. Mol. Cell Biol.* **2011**, *12*, 295−307.
(8) Matsumoto, M. L.; Wickliffe, K. E.; Dong, K. C.; Yu, C.; Bosanac, I.; Bustos, D.; Phu, L.; Kirkpatrick, D. S.; Hymowitz, S. G.; Rape, M. K11-linked polyubiquitination in cell cycle control revealed by a K11 linkage-specific antibody. *Mol. Cell* **2010**, *39*, 477−484.
(9) Pines, J. Cubism and the cell cycle: the many faces of the APC/C. *Nat. Rev. Mol. Cell Biol.* **2011**, *12*, 427−438.
(10) Nakada, S.; Tai, I.; Panier, S.; Al-Hakim, A.; Iemura, S.-i.; Juang, Y.-C.; O'Donnell, L.; Kumakubo, A.; Munro, M.; Sicheri, F. Non-canonical inhibition of DNA damage-dependent ubiquitination by OTUB1. *Nature* **2010**, *466*, 941−946.
(11) Nakazawa, Y.; Hara, Y.; Oka, Y.; Komine, O.; van den Heuvel, D.; Guo, C.; Daigaku, Y.; Isono, M.; He, Y.; Shimada, M.; Kato, K.; Jia, N.; Hashimoto, S.; Kotani, Y.; Miyoshi, Y.; Tanaka, M.; Sobue, A.; Mitsutake, N.; Suganami, T.; Masuda, A.; Ohno, K.; Nakada, S.; Mashimo, T.; Yamanaka, K.; Luijsterburg, S. M.; Ogi, T. Ubiquitination of DNA damage-stalled RNAPII promotes transcription-coupled repair. *Cell* **2020**, *180*, 1228−1244.
(12) Yau, R. G.; Doerner, K.; Castellanos, E. R.; Haakonsen, D. L.; Werner, A.; Wang, N.; Yang, X. W.; Martinez-Martin, N.; Matsumoto, M. L.; Dixit, V. M.; Rape, M. Assembly and function of heterotypic ubiquitin chains in cell-cycle and protein quality control. *Cell* **2017**, *171*, 918−933.
(13) Samant, R. S.; Livingston, C. M.; Sontag, E. M.; Frydman, J. Distinct proteostasis circuits cooperate in nuclear and cytoplasmic protein quality control. *Nature* **2018**, *563*, 407−411.
(14) Popovic, D.; Vucic, D.; Dikic, I. Ubiquitination in disease pathogenesis and treatment. *Nat. Med.* **2014**, *20*, 1242−1253.
(15) van Twest, S.; Murphy, V. J.; Hodson, C.; Tan, W.; Swuec, P.; O'Rourke, J. J.; Heierhorst, J.; Crismani, W.; Deans, A. J. Mechanism of ubiquitination and deubiquitination in the Fanconi anemia pathway. *Mol. Cell* **2017**, *65*, 247−259.
(16) Knies, K.; Inano, S.; Ramírez, M. J.; Ishiai, M.; Surrallés, J.; Takata, M.; Schindler, D. Biallelic mutations in the ubiquitin ligase RFWD3 cause Fanconi anemia. *J. Clin. Invest.* **2017**, *127*, 3013−3027.
(17) Shimura, H.; Schlossmacher, M. G.; Hattori, N.; Frosch, M. P.; Trockenbacher, A.; Schneider, R.; Mizuno, Y.; Kosik, K. S.; Selkoe, D. J. Ubiquitination of a new form of α-synuclein by parkin from human brain: implications for Parkinson's disease. *Science* **2001**, *293*, 263−269.
(18) Nakayama, K. I.; Nakayama, K. Ubiquitin ligases: cell-cycle control and cancer. *Nat. Rev. Cancer* **2006**, *6*, 369−381.
(19) Xu, G.; Paige, J. S.; Jaffrey, S. R. Global analysis of lysine ubiquitination by ubiquitin remnant immunoaffinity profiling. *Nat. Biotechnol.* **2010**, *28*, 868−873.
(20) Akimov, V.; Barrio-Hernandez, I.; Hansen, S. V.; Hallenborg, P.; Pedersen, A.-K.; Bekker-Jensen, D. B.; Puglia, M.; Christensen, S. D.; Vanselow, J. T.; Nielsen, M. M.; Kratchmarova, I.; Kelstrup, C. D.; Olsen, J. V.; Blagoev, B. UbiSite approach for comprehensive mapping of lysine and N-terminal ubiquitination sites. *Nat. Struct. Mol. Biol.* **2018**, *25*, 631−640.
(21) Davies, C. W.; Vidal, S. E.; Phu, L.; Sudhamsu, J.; Hinkle, T. B.; Chan Rosenberg, S.; Schumacher, F.-R.; Zeng, Y. J.; Schwerdtfeger, C.; Peterson, A. S. Antibody toolkit reveals N-terminally ubiquitinated substrates of UBE2W. *Nat. Commun.* **2021**, *12*, 4608.
(22) Yu, Y.; Zheng, Q.; Erramilli, S. K.; Pan, M.; Park, S.; Xie, Y.; Li, J.; Fei, J.; Kossiakoff, A. A.; Liu, L.; Zhao, M. K29-linked ubiquitin signaling regulates proteotoxic stress response and cell cycle. *Nat. Chem. Biol.* **2021**, *17*, 896−905.
(23) Michel, M. A.; Swatek, K. N.; Hospenthal, M. K.; Komander, D. Ubiquitin linkage-specific affimers reveal insights into K6-linked ubiquitin signaling. *Mol. Cell* **2017**, *68*, 233−246.
(24) Hjerpe, R.; Aillet, F.; Lopitz-Otsoa, F.; Lang, V.; England, P.; Rodriguez, M. S. Efficient protection and isolation of ubiquitylated proteins using tandem ubiquitin-binding entities. *EMBO Rep.* **2009**, *10*, 1250−1258.
(25) Yoshida, Y.; Saeki, Y.; Murakami, A.; Kawawaki, J.; Tsuchiya, H.; Yoshihara, H.; Shindo, M.; Tanaka, K. A comprehensive method for detecting ubiquitinated substrates using TR-TUBE. *Proc. Natl. Acad. Sci. U. S. A.* **2015**, *112*, 4630−4635.
(26) Gao, Y.; Li, Y.; Zhang, C.; Zhao, M.; Deng, C.; Lan, Q.; Liu, Z.; Su, N.; Wang, J.; Xu, F.; Xu, Y.; Ping, L.; Chang, L.; Gao, H.; Wu, J.; Xue, Y.; Deng, Z.; Peng, J.; Xu, P. Enhanced purification of ubiquitinated proteins by engineered tandem hybrid ubiquitin-binding domains (ThUBDs). *Mol. Cell Proteomics* **2016**, *15*, 1381−1396.
(27) Xiao, W.; Liu, Z.; Luo, W.; Gao, Y.; Chang, L.; Li, Y.; Xu, P. Specific and unbiased detection of polyubiquitination via a sensitive non-antibody approach. *Anal. Chem.* **2020**, *92*, 1074−1080.
(28) Min, M.; Mayor, U.; Dittmar, G.; Lindon, C. Using in vivo biotinylated ubiquitin to describe a mitotic exit ubiquitome from human cells. *Mol. Cell Proteomics* **2014**, *13*, 2411−2425.
(29) Akimov, V.; Henningsen, J.; Hallenborg, P.; Rigbolt, K. T.; Jensen, S. S.; Nielsen, M. M.; Kratchmarova, I.; Blagoev, B. StUbEx: stable tagged ubiquitin exchange system for the global investigation of cellular ubiquitination. *J. Proteome Res.* **2014**, *13*, 4192−4204.
(30) Kliza, K.; Taumer, C.; Pinzuti, I.; Franz-Wachtel, M.; Kunzelmann, S.; Stieglitz, B.; Macek, B.; Husnjak, K. Internally tagged ubiquitin: a tool to identify linear polyubiquitin-modified proteins by mass spectrometry. *Nat. Methods* **2017**, *14*, 504−512.
(31) Lee, I.; Schindelin, H. Structural insights into E1-catalyzed ubiquitin activation and transfer to conjugating enzymes. *Cell* **2008**, *134*, 268−278.
(32) Lv, Z.; Williams, K. M.; Yuan, L.; Atkison, J. H.; Olsen, S. K. Crystal structure of a human ubiquitin E1−ubiquitin complex reveals conserved functional elements essential for activity. *J. Biol. Chem.* **2018**, *293*, 18337−18352.
(33) Billington, A. P.; Walstrom, K. M.; Ramesh, D.; Guzikowski, A. P.; Carpenter, B. K.; Hess, G. P. Synthesis and photochemistry of photolabile N-glycine derivatives and effects of one on the glycine receptor. *Biochemistry* **1992**, *31*, 5500−5507.
(34) Wu, N.; Deiters, A.; Cropp, T. A.; King, D.; Schultz, P. G. A genetically encoded photocaged amino acid. *J. Am. Chem. Soc.* **2004**, *126*, 14306−14307.
(35) Deiters, A.; Groff, D.; Ryu, Y.; Xie, J.; Schultz, P. G. A genetically encoded photocaged tyrosine. *Angew. Chem., Int. Ed.* **2006**, *45*, 2728−2731.
(36) Ohmuro-Matsuyama, Y.; Tatsu, Y. Photocontrolled cell adhesion on a surface functionalized with a caged arginine-glycine-aspartate peptide. *Angew. Chem., Int. Ed.* **2008**, *47*, 7527−7529.
(37) Salveson, P. J.; Haerianardakani, S.; Thuy-Boun, A.; Kreutzer, A. G.; Nowick, J. S. Controlling the oligomerization state of Aβ-derived peptides with light. *J. Am. Chem. Soc.* **2018**, *140*, 5842−5852.
(38) van der Leun, A. M.; Hoekstra, M. E.; Reinalda, L.; Scheele, C. L.; Toebes, M.; van de Graaff, M. J.; Chen, L. Y.; Li, H.; Bercovich, A.; Lubling, Y.; David, E.; Thommen, D. S.; Tanay, A.; Rheenen, J. V.; Amit, I.; Kasteren, S. I. V.; Schumacher, T. N. Single-cell analysis of regions of interest (SCARI) using a photosensitive tag. *Nat. Chem. Biol.* **2021**, *17*, 1139−1147.
(39) Mondal, S.; Wang, S.; Zheng, Y.; Sen, S.; Chatterjee, A.; Thompson, P. R. Site-specific incorporation of citrulline into proteins in mammalian cells. *Nat. Commun.* **2021**, *12*, 45.

https://doi.org/10.1021/jacsau.3c00421
JACS Au 2023, 3, 2873−2882

(40) Wang, J.; Liu, Y.; Liu, Y.; Zheng, S.; Wang, X.; Zhao, J.; Yang, F.; Zhang, G.; Wang, C.; Chen, P. R. Time-resolved protein activation by proximal decaging in living systems. *Nature* **2019**, *569*, 509−513.
(41) Ruskowitz, E. R.; Munoz-Robles, B. G.; Strange, A. C.; Butcher, C. H.; Kurniawan, S.; Filteau, J. R.; DeForest, C. A. Spatiotemporal functional assembly of split protein pairs through a light-activated SpyLigation. *Nat. Chem.* **2023**, *15*, 694−704, DOI: 10.1038/s41557-023-01152-x.
(42) Liu, J.; Chen, H.; Ma, L.; He, Z.; Wang, D.; Liu, Y.; Lin, Q.; Zhang, T.; Gray, N.; Kaniskan, H. Ü.; Jin, J.; Wei, W. Light-induced control of protein destruction by opto-PROTAC. *Sci. Adv.* **2020**, *6*, No. eaay5154.
(43) Khosla, M.; Smeby, R.; Bumpus, F. Failure sequence in solid-phase peptide synthesis due to the presence of an N-alkylamino acid. *J. Am. Chem. Soc.* **1972**, *94*, 4721−4724.
(44) Fernández-Llamazares, A. I.; Spengler, J.; Albericio, F. Review backbone N-modified peptides: How to meet the challenge of secondary amine acylation. *Pept. Sci.* **2015**, *104*, 435−452.
(45) Liang, L. J.; Chu, G. C.; Qu, Q.; Zuo, C.; Mao, J.; Zheng, Q.; Chen, J.; Meng, X.; Jing, Y.; Deng, H.; Li, Y. M.; Liu, L. Chemical synthesis of activity-based E2-ubiquitin probes for the structural analysis of E3 ligase-catalyzed transthiolation. *Angew. Chem., Int. Ed.* **2021**, *60*, 17171−17177.
(46) Stewart, M. D.; Ritterhoff, T.; Klevit, R. E.; Brzovic, P. S. E2 enzymes: more than just middle men. *Cell Res.* **2016**, *26*, 423−440.
(47) Buetow, L.; Huang, D. T. Structural insights into the catalysis and regulation of E3 ubiquitin ligases. *Nat. Rev. Mol. Cell Biol.* **2016**, *17*, 626−642.
(48) Herce, H. D.; Schumacher, D.; Schneider, A. F.; Ludwig, A. K.; Mann, F. A.; Fillies, M.; Kasper, M.-A.; Reinke, S.; Krause, E.; Leonhardt, H.; Cardoso, M. C.; Hackenberger, C. P. Cell-permeable nanobodies for targeted immunolabelling and antigen manipulation in living cells. *Nat. Chem.* **2017**, *9*, 762−771.
(49) Schneider, A. F.; Kithil, M.; Cardoso, M. C.; Lehmann, M.; Hackenberger, C. P. Cellular uptake of large biomolecules enabled by cell-surface-reactive cell-penetrating peptide additives. *Nat. Chem.* **2021**, *13*, 530−539.
(50) Mandal, S.; Mann, G.; Satish, G.; Brik, A. Enhanced live-cell delivery of synthetic proteins assisted by cell-penetrating peptides fused to DABCYL. *Angew. Chem., Int. Ed.* **2021**, *60*, 7333−7343.
(51) Saha, A.; Mandal, S.; Arafiles, J. V. V.; Gómez-González, J.; Hackenberger, C. P.; Brik, A. Structure-Uptake Relationship Study of DABCYL Derivatives Linked to Cyclic Cell-Penetrating Peptides for Live-Cell Delivery of Synthetic Proteins. *Angew. Chem., Int. Ed.* **2022**, *61*, No. e202207551.
(52) Shang, F.; Taylor, A. Ubiquitin−proteasome pathway and cellular responses to oxidative stress. *Free Radical Biol. Med.* **2011**, *51*, 5−16.
(53) Silva, G. M.; Finley, D.; Vogel, C. K63 polyubiquitination is a new modulator of the oxidative stress response. *Nat. Struct. Mol. Biol.* **2015**, *22*, 116−123.
(54) Maxwell, B. A.; Gwon, Y.; Mishra, A.; Peng, J.; Nakamura, H.; Zhang, K.; Kim, H. J.; Taylor, J. P. Ubiquitination is essential for recovery of cellular activities after heat shock. *Science* **2021**, *372*, No. eabc3593.
(55) Huang, D. W.; Sherman, B. T.; Lempicki, R. A. Systematic and integrative analysis of large gene lists using DAVID bioinformatics resources. *Nat. Protoc.* **2009**, *4*, 44−57.
(56) Tolay, N.; Buchberger, A. Comparative profiling of stress granule clearance reveals differential contributions of the ubiquitin system. *Life Sci. Alliance* **2021**, *4*, No. e202000927.
(57) Zhang, Y.; Hirota, T.; Kuwata, K.; Oishi, S.; Gramani, S. G.; Bode, J. W. Chemical Synthesis of Atomically Tailored SUMO E2 Conjugating Enzymes for the Formation of Covalently Linked SUMO-E2-E3 Ligase Ternary Complexes. *J. Am. Chem. Soc.* **2019**, *141*, 14742−14751.
(58) Ai, H.; Sun, M.; Liu, A.; Sun, Z.; Liu, T.; Cao, L.; Liang, L.; Qu, Q.; Li, Z.; Deng, Z.; Tong, Z.; Chu, G.; Tian, X.; Deng, H.; Zhao, S.; Li, J.-B.; Lou, Z.; Liu, L. H2B Lys34 ubiquitination induces nucleosome distortion to stimulate Dot1L activity. *Nat. Chem. Biol.* **2022**, *18*, 972−980.
(59) Mann, G.; Satish, G.; Meledin, R.; Vamisetti, G. B.; Brik, A. Palladium-Mediated Cleavage of Proteins with Thiazolidine-Modified Backbone in Live Cells. *Angew. Chem., Int. Ed.* **2019**, *58*, 13540−13549.
(60) Ai, H.; Chu, G.-C.; Gong, Q.; Tong, Z.; Deng, Z.; Liu, X.; Yang, F.; Xu, Z.; Li, J.-B.; Tian, C.; Liu, L. Chemical synthesis of post-translationally modified H2AX reveals redundancy in interplay between histone phosphorylation, ubiquitination, and methylation on the binding of 53BP1 with nucleosomes. *J. Am. Chem. Soc.* **2022**, *144*, 18329−18337.
(61) Tolmachova, K. A.; Farnung, J.; Liang, J. R.; Corn, J. E.; Bode, J. W. Facile Preparation of UFMylation Activity-Based Probes by Chemoselective Installation of Electrophiles at the C-Terminus of Recombinant UFM1. *ACS Cent. Sci.* **2022**, *8*, 756−762.
(62) Li, C.; Wang, T.; Liang, L.; Chu, G.; Zhang, J.; He, W.; Liu, L.; Li, J. Simultaneous capture of ISG15 conjugating and deconjugating enzymes using a semi-synthetic ISG15-Dha probe. *Sci. China Chem.* **2023**, *66*, 837−844.
(63) Gui, W.; Shen, S.; Zhuang, Z. Photocaged cell-permeable ubiquitin probe for temporal profiling of deubiquitinating enzymes. *J. Am. Chem. Soc.* **2020**, *142*, 19493−19501.
(64) Farnung, J.; Muhar, M.; Liang, J. R.; Tolmachova, K. A.; Benoit, R. M.; Corn, J. E.; Bode, J. W. Semisynthetic LC3 Probes for Autophagy Pathways Reveal a Noncanonical LC3 Interacting Region Motif Crucial for the Enzymatic Activity of Human ATG3. *ACS Cent. Sci.* **2023**, *9*, 1025−1034.
(65) Ai, H.; Tong, Z.; Deng, Z.; Tian, J.; Zhang, L.; Sun, M.; Du, Y.; Xu, Z.; Shi, Q.; Liang, L.; Zheng, Q.; Li, J.-B.; Pan, M.; Liu, L. Synthetic E2-Ub-nucleosome conjugates for studying nucleosome ubiquitination. *Chem* **2023**, *9*, 1221−1240.
(66) Gui, W.; Ott, C. A.; Yang, K.; Chung, J. S.; Shen, S.; Zhuang, Z. Cell-permeable activity-based ubiquitin probes enable intracellular profiling of human deubiquitinases. *J. Am. Chem. Soc.* **2018**, *140*, 12424−12433.
(67) Mangubat-Medina, A. E.; Ball, Z. T. Triggering biological processes: Methods and applications of photocaged peptides and proteins. *Chem. Soc. Rev.* **2021**, *50*, 10403−10421.
(68) Wang, Y.; Chen, J.; Hua, X.; Meng, X.; Cai, H.; Wang, R.; Shi, J.; Deng, H.; Liu, L.; Li, Y. M. Photocaging of Activity-Based Ubiquitin Probes via a C-Terminal Backbone Modification Strategy. *Angew. Chem., Int. Ed.* **2022**, *61*, No. e202203792.

https://doi.org/10.1021/jacsau.3c00421
JACS Au 2023, 3, 2873−2882